

A split-and-transfer flow based entropic centrality

Frédérique Oggier^{Equal first author, 1}, **Silivanxay Phetsouvanh**², **Anwitaman Datta**^{Corresp. Equal first author, 2}

¹ Division of Mathematical Sciences, Nanyang Technological University, Singapore, Singapore

² School of Computer Science and Engineering, Nanyang Technological University, Singapore, Singapore

Corresponding Author: Anwitaman Datta
Email address: anwitaman@ntu.edu.sg

The notion of entropic centrality measures how central a node is in terms of how uncertain the destination of a flow starting at this node is: the more uncertain the destination, the more well connected and thus central the node is deemed. This implicitly assumes that the flow is indivisible, and at every node, the flow is transferred from one edge to another. The contribution of this paper is to propose a split-and-transfer flow model for entropic centrality, where at every node, the flow can actually be arbitrarily split across choices of neighbours. We show how to map this to an equivalent transfer entropic centrality set-up for the ease of computation, and carry out three case studies (an airport network, a cross-shareholding network and a Bitcoin transactions subnetwork) to illustrate the interpretation and insights linked to this new notion of centrality.

A Split-and-Transfer Flow Based Entropic Centrality

Frédérique Oggier¹, Silivanxay Phetsouvanh², and Anwitaman Datta²

¹Division of Mathematical Sciences, Nanyang Technological University, Singapore

²School of Computer Science and Engineering, Nanyang Technological University, Singapore

Corresponding author:

Anwitaman Datta¹

Email address: anwitaman@ntu.edu.sg

ABSTRACT

The notion of entropic centrality measures how central a node is in terms of how uncertain the destination of a flow starting at this node is: the more uncertain the destination, the more well connected and thus central the node is deemed. This implicitly assumes that the flow is indivisible, and at every node, the flow is transferred from one edge to another. The contribution of this paper is to propose a split-and-transfer flow model for entropic centrality, where at every node, the flow can actually be arbitrarily split across choices of neighbors. We show how to map this to an equivalent transfer entropic centrality set-up for the ease of computation, and carry out two case studies, a cross-shareholding network and a Bitcoin transactions subnetwork, to illustrate the interpretation and insights linked to this new notion of centrality.

1 INTRODUCTION

Centrality is a classical measure used in graph theory and network analysis to identify important vertices. The meaning of “important” depends on the nature of the problem analyzed, e.g. hubs in networks, spreaders of a disease, or influencers in social networks. Commonly used centrality measures include: the *degree centrality* which is the degree (or in-degree/out-degree) of the vertex depending on whether the graph is directed, possibly normalized to get the fraction of vertices a given vertex is connected to; the *closeness centrality* which is the reciprocal of the sum of the shortest path distances from a given vertex to all others, typically normalized, and indicates how close a given vertex is to all other vertices in the network; the *betweenness centrality* which is the sum of the fraction of all pairs of shortest paths that pass through it, indicating the extent to which a given vertex stands between other vertex pairs (see e.g. Estrada (2011) for a survey of different centrality measures and how centralities fit into the more general framework of complex networks). These were extended to weighted graphs, though at the risk of changing the interpretation of the measure, e.g., one may use weighted degrees instead of degrees, but this measure does not count the number of neighbors anymore (see e.g. Opsahl et al. (2010) for a discussion on using the above cited centrality measures for weighted graphs). Another way to determine centrality is to assign as centrality a (scaled) average of the centralities of the neighbors. This is the idea behind *eigenvector centrality* discussed by Newman (2009), which was already debated by Bonacich (1972), who later generalized it to *alpha centrality* (Bonacich and Lloyd (2001)). Alpha centrality introduces an additive exogenous term, which accounts for an influencing factor which does not depend on the network structure. Though *Katz centrality* (Katz (1953)) relies on the idea that importance is measured by weighted numbers of walks from the vertex in question to other vertices (where longer walks have less weights than short ones), it turns out that the alpha centrality and Katz centrality differ by a constant term. With these three centralities, a highly central vertex with many links tends to endorse all its neighbors which in turn become highly central. However one could argue that the inherited centrality should be diluted if the central vertex is too magnanimous in the sense that it has too many neighbors. This is solved by Page Rank centrality, which is based on the *PageRank* algorithm developed by Page et al. (1999). Benzi and Klymko (2015) showed that a parameterized random walk model can capture the behavior of a gamut of centrality measures, including degree centrality (walks of length one) and eigenvector based

47 centrality models (considered as infinite walks), which contain the eigenvector and Katz centralities as
48 particular cases. This parameterized model helps explain and interpret the high rank correlation observed
49 among degree centrality and eigenvector based centralities.

50 Notwithstanding this high rank correlation among centrality measures, each measure captures the
51 vertex importance subject to a certain interpretation of importance, which is a key rationale behind
52 studying different centrality models in different contexts. A seminal work by Borgatti (2005) looked
53 at which notion of centrality is best suited given a scenario, by characterizing the scenario as a flow
54 circulating over a network: a typology of the flow process is given across two dimensions, the type
55 of circulation (parallel/serial duplication, transfer) and the flow trajectories (geodesics, paths, trails, or
56 walks): a flow may be based on *transfer*, where an item or unit flows in an indivisible manner (e.g.,
57 package delivery), or by serial replication, in which both the node that sends the item and the one that
58 receives it have the item (e.g., one-to-one gossip), or parallel duplication, where an item can be transmitted
59 in parallel through all outgoing edges (e.g., epidemic spread). It was shown for example that betweenness
60 is best suited for geodesics and transfer, while eigenvector based centralities should be used for walks and
61 parallel duplication. Indeed, betweenness is based on shortest paths, suggesting a target to be reached
62 as fast as possible, and thus fitting transfer. Using Katz's intuition, eigenvector based centralities count
63 possible unconstrained walks, and they are consistent with a scenario where every vertex influences all of
64 its neighbors simultaneously, which is consistent with parallel deduplication. This flow characterization is
65 of interest for this work, since we will be looking at a case where a flow is actually not just transferred,
66 but also split among outgoing edges, with the possibility to partly remain at any node it encounters. This
67 scenario could typically be motivated by financial transactions, which are transferred, not duplicated.
68 However when transferred, the flow of money is not indivisible. Based on Borgatti's typology, a measure
69 of centrality for transfer should be based on paths rather than eigenvectors. This is indeed the approach
70 that we will explore.

Our starting point is the notion of entropic centrality as proposed by Tutzauer (2007). A (directed)
graph $G = (V, E)$ with vertex set V and edge set E is built whose edges are unweighted. To define the
centrality of $u \in V$, the probability $p_{u,v}$ that a random walk constrained to not revisit any vertex (thus, only
forming paths) starting at u terminates at v is computed. To model the stoppage of flow/walk at any vertex,
an edge to itself (self-loop) is added. The process of computing $p_{u,v}$ is thus to consider a constrained
random walk to start at node u , and at every node w encountered in the path, to choose an outgoing edge
uniformly at random among the edges leading to unvisited nodes (or choosing the self-loop to terminate
the walk). Then the entropic centrality $C_H(u)$ of u is defined to be

$$C_H(u) = - \sum_{v \in V} p_{u,v} \log_2 p_{u,v}. \quad (1)$$

71 This notion of entropic centrality was adapted in Nikolaev et al. (2015) to fit a Markov model, where
72 instead of paths, unconstrained random walks are considered, for computational efficiency. In general,
73 how to compute centrality at scale is an interesting direction of study in its own right, e.g. Fan et al.
74 (2017), but this is somewhat orthogonal to the emphasis of the current work.

75 In this work we revisit and generalize the original concept of entropic centrality to make it more
76 flexible. To do so, we first interpret the "transfer" centrality proposed in Tutzauer (2007) as having (1) an
77 underlying graph, where every edge has a probability which is that of being chosen uniformly at random
78 among the other outgoing edges of a given vertex, and (2) an indivisible flow which starts at a vertex u ,
79 and follows some path where the probability to choose an edge at every vertex in this path is given by the
80 probability attached to this edge, taking into account unvisited neighbors, to reach v . Since the flow is
81 indivisible, the self-loop represents the probability for this flow to stop at a given vertex.

82 In our generalization, we similarly assume that we have (1) an underlying graph, only now the
83 probability attached to each edge depends on the scenario considered and could be arbitrary, (2) the flow
84 used to measure centrality can split among neighbors, by specifying which subsets it goes to with which
85 probability, at every vertex it encounters (as per a *flow* in the traditional network analysis sense, flow
86 conservation applies, meaning that the amount of flow that goes out of u is the same amount of flow that
87 reaches all of its neighbors). Again, a self-loop is an artifact introduced to capture the effect of the flow
88 on vertices, even if none of the flow actually remains in the vertex (As in (Nikolaev et al. (2015)), a zero
89 probability would otherwise render zero contribution to the entropic centrality calculation). While the
90 underlying phenomenon may have self-loops, they may or not be directly used to determine the self-loops
91 needed for the mathematical model. This should be determined based on the scenario being modeled.

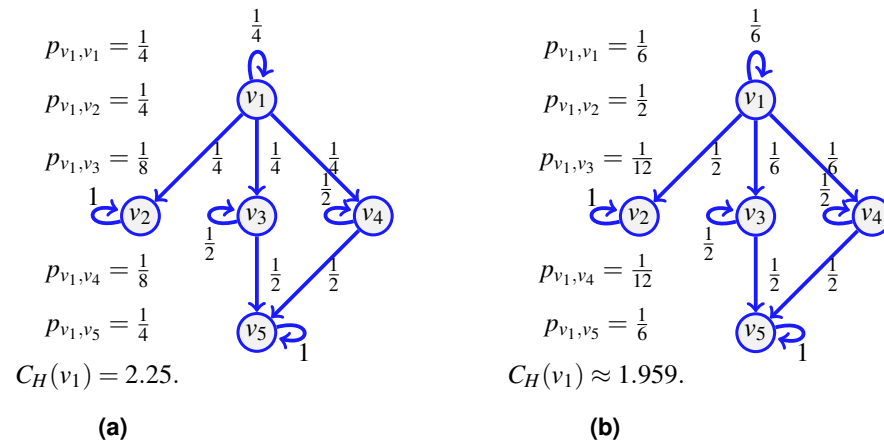


Figure 1. The transfer entropic centrality $C_H(v_1)$ of v_1 is computed using (1), for a uniform edge distribution (the choice of an edge at a given vertex is chosen uniformly at random among choices of unvisited neighbors) in (1a), and for a non-uniform distribution in (1b).

92 The above motivates the notion of a *split-and-transfer* entropic centrality. Since propagation of flow
 93 is an indicator of spread over the network, we will also consider a scaled version of entropic centrality,
 94 where a multiplicative factor is introduced to incorporate additional information, which may suggest an a
 95 priori difference of importance among the vertices, for instance, if the data suggests that some vertices
 96 handle volume of goods much larger than other vertices.

97 The contributions of this work are to (1) introduce the above framework for split-and-transfer entropic
 98 centrality, (2) show in Subsection 2.1 that transfer centrality can be easily extended to consider arbitrary
 99 probabilities on graph edges and (3) prove that computing the split-and-transfer entropic centrality can be
 100 reduced to transfer entropic centrality over a graph with suitable equivalent edge probabilities (which
 101 is crucial from a practicality perspective), as shown in Proposition 1 of Subsection 2.1. Two studies
 102 that showcase and explore our technique are provided in Section 3: (i) a cross-shareholding network
 103 representing portfolio diversification, used to showcase the versatility of our framework and (ii) a subgraph
 104 of wallet addresses from the Bitcoin network, which originally motivated us to study the notion of subsets
 105 for split-and-transfer flows. Comparisons with other standard centralities (alpha, Katz, betweenness and
 106 PageRank) are given, showing that the entropic centrality captures different features.

107 2 THE NOTION OF SPLIT-AND-TRANSFER ENTROPIC CENTRALITY

108 2.1 The Transfer Entropic Centrality

109 Consider the network shown on Figure 1a and assume that the probability of an indivisible flow going
 110 from one vertex to another is uniform at random (including the option to remain at the current vertex).
 111 For a flow starting at v_1 , there is then a probability $\frac{1}{4}$ to go to v_4 , and a probability $\frac{1}{2}$ to continue to v_5 , so
 112 the probability to go from v_1 to v_5 following the path (v_1, v_4, v_5) is $\frac{1}{8}$. But since it is also possible to reach
 113 v_5 from v_1 using v_3 instead, an event of probability $\frac{1}{8}$, we have that the probability p_{v_1, v_5} for an indivisible
 114 flow to start at v_1 and stop at v_5 is $p_{v_1, v_5} = \frac{1}{4}$. Similarly, we compute p_{v_1, v_1} , p_{v_1, v_2} , p_{v_1, v_3} and p_{v_1, v_4} , and
 115 the transfer entropic centrality $C_H(u)$ of $u = v_1$ is $C_H(v_1) = \frac{3}{4} \log_2 4 + \frac{2}{8} \log_2(8) = 2.25$ by (1).

116 For a point of comparison, on the right of the same figure, we change the probability to go out of v_1 ,
 117 such that the edge (v_1, v_2) is chosen with a probability $\frac{1}{2}$, while the probability is $\frac{1}{6}$ for using the edges to
 118 the other vertices (including a probability $\frac{1}{6}$ that the flow just stays at v_1 itself). The resulting probabilities
 119 are provided on Figure 1b. There is no complication in computing $C_H(v_1)$ using (1) with non-uniform
 120 probabilities. This reduces slightly the centrality of v_1 , which is consistent with the interpretation of
 121 entropic centrality: the underlying notion of entropy is a measure of uncertainty (Tutzauer (2007)), the
 122 uncertainty of the final destination of a flow, knowing that it started at a given vertex. Imagine the
 123 most extreme case where the edge (v_1, v_2) is chosen with a probability 1, then even though v_1 has three
 124 potential outgoing neighbors, two of them are used with probability 0, so the centrality of v_1 would reduce
 125 considerably, as expected, since there is no uncertainty left regarding the destination of a flow at v_1 .

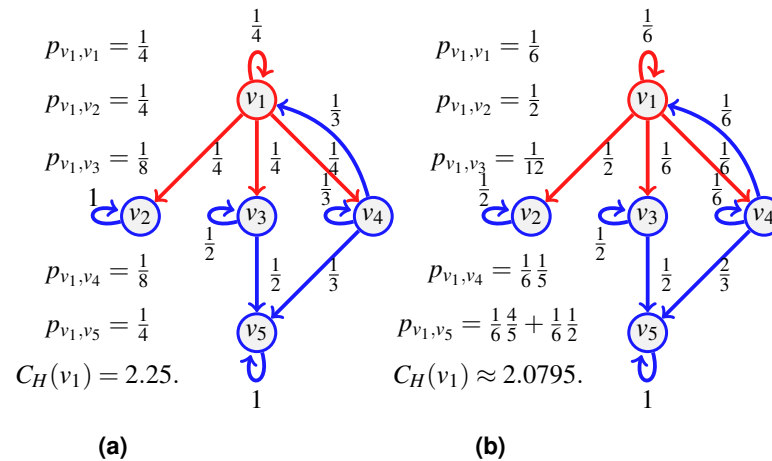


Figure 2. An example of transfer centrality involving already visited neighbors. If probabilities are uniform at random (2a), they are scaled according to the number of unvisited neighbors. If not (2b), they are scaled proportionally to the existing probabilities.

126 The notion of transfer entropic centrality captured by (1) assumes that there is no vertex repetition
 127 in the paths taken by the flow. Figure 2 illustrates this hypothesis. Again for the centrality of v_1 , a flow
 128 leaves v_1 , it can go to either v_2 , v_3 or v_4 . When reaching v_4 , the flow cannot go back to v_1 , since v_1
 129 is already visited (and going back would not give a path anymore), there the probabilities to stay at v_4
 130 and to go to v_5 from v_4 are modified. On the left, when probabilities are uniform, since now only two
 131 outgoing edges of v_4 are available, namely edges (v_4, v_4) and (v_4, v_5) , each is assigned a probability of $\frac{1}{2}$.
 132 On the right, when probabilities are not uniform, we distribute the probability of going to some visited
 133 vertex proportionally to the rest of the available edges. Since $\frac{4}{6}$ is going to v_5 while $\frac{1}{6}$ is staying at v_4 , we
 134 have 4 and 1 out of 5 respectively leaving and staying, thus obtaining the renormalized probabilities as
 135 $\frac{4}{6} + \frac{4}{5} \frac{1}{6} = \frac{4}{5}$ and $\frac{1}{6} + \frac{1}{5} \frac{1}{6} = \frac{1}{5}$.

136 The examples of Figures 1 and 2 illustrate diverse cases of indivisible flow. By definition of indivis-
 137 ibility, the choice of an edge at a vertex u corresponds to choosing subsets containing one vertex only
 138 in the list of all subsets of neighbors. We can thus set a probability 0 to all subsets which contain more
 139 than one vertex. Therefore, the definition of entropic centrality in (1), with or without uniform edge
 140 probabilities, are particular cases of the proposed split-and-transfer framework, that we discuss next.

141 2.2 The Split-and-Transfer Entropic Centrality

142 Consider the network of Figure 3 depicting a seller v_1 whose direct customers are v_2, v_3, v_4 . Say we
 143 further know that when v_1 distributes a new batch of items, he does so to either customers $\{v_2, v_3\}$ or
 144 $\{v_3, v_4\}$, and in fact, the pair $\{v_3, v_4\}$ is preferred (they receive $\frac{2}{3}$ of the batches, versus $\frac{1}{3}$ for the
 145 group $\{v_2, v_3\}$). Furthermore, in the first case, v_2 receives a higher volume than v_3 (say $\frac{2}{3}$ of the batch
 146 goes to v_2), while for the second case, v_4 takes $\frac{3}{4}$ of the batch shared with v_3 . Once v_3, v_4 obtain
 147 the items, they typically keep half for themselves, and distribute the other half to v_5 . To compute the
 148 centrality of v_1 , we consider a divisible flow starting at $u = v_1$ which can split among different paths
 149 instead of following one. To model the choice of splitting among possible neighbors, we first define a
 150 probability $q(x)$ over the set $\mathcal{E}_u = \{ \{v_1\}, \{v_2\}, \{v_3\}, \{v_4\}, \{v_1, v_2\}, \{v_1, v_3\}, \{v_1, v_4\}, \{v_2, v_3\}, \{v_2, v_4\},$
 151 $\{v_3, v_4\}, \{v_1, v_2, v_3\}, \{v_1, v_2, v_4\}, \{v_1, v_3, v_4\}, \{v_2, v_3, v_4\}, \{v_1, v_2, v_3, v_4\} \}$ such that, for our example,
 152 $q(\{v_2, v_3\}) = \frac{1}{3}$, $q(\{v_3, v_4\}) = \frac{2}{3}$, and $q(x) = 0$ for other choices of x (in contrast to (Oggier et al. (2018))
 153 where it was chosen to be uniformly at random). This represents the fact that $\frac{1}{3}$ of the time, v_1 sends the
 154 goods to the pair $\{v_2, v_3\}$, while for the rest of the time, it sends it to the pair $\{v_3, v_4\}$. We compute the
 155 path probabilities for each event, for $q(\{v_2, v_3\}) = \frac{1}{3}$ on the left of Figure 3, and for $q(\{v_3, v_4\}) = \frac{2}{3}$ on
 156 the right. We have further information: when v_1 deals with $\{v_2, v_3\}$, there is a bias of $\frac{2}{3}$ for v_2 compared
 157 to $\frac{1}{3}$ for v_3 , and the bias is of $\frac{3}{4}$ for v_4 in the other case. The corresponding probabilities are attached to the
 158 edges $\{(v_1, v_2), (v_1, v_3)\}$ and $\{(v_1, v_3), (v_1, v_4)\}$ respectively. Now that the edge probabilities are defined,
 159 we can compute the path probabilities. For example, from v_1 to v_5 , we sum up the path probabilities for

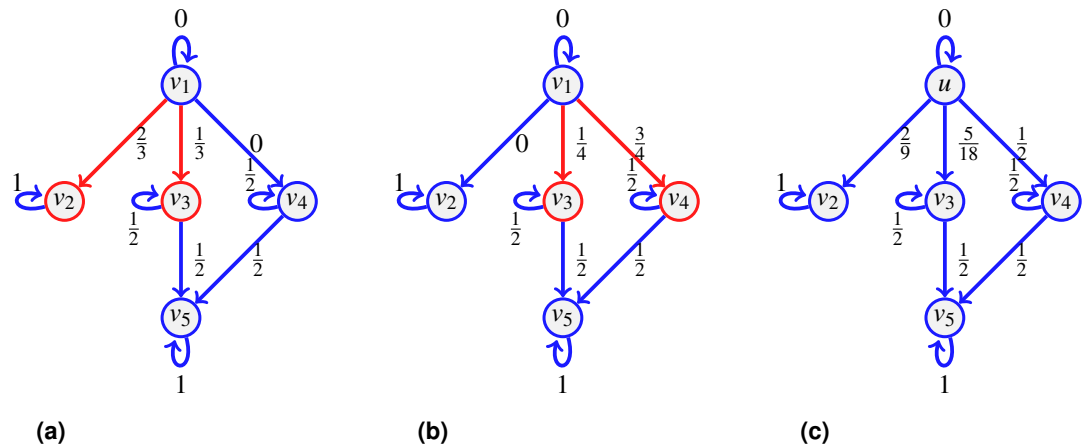


Figure 3. An example of split-and-transfer entropic centrality: on (3a) in red, the event corresponding to choosing $\{v_2, v_3\}$, in (3b), the event $\{v_3, v_4\}$. The probabilities $p_{u,v}$ are computed by summing over both events, weighted by the respective event probability: $p_{v_1, v_2} = \frac{1}{3}(\frac{2}{3}) = \frac{2}{9}$, $p_{v_1, v_4} = \frac{2}{3}(\frac{3}{8}) = \frac{1}{4}$, $p_{v_1, v_3} = \frac{1}{3}(\frac{1}{6}) + \frac{2}{3}(\frac{1}{8})$, $p_{v_1, v_5} = \frac{1}{3}(\frac{1}{6}) + \frac{2}{3}(\frac{1}{8} + \frac{3}{8})$. This gives $C_H(v_1) \approx 1.9076$.

160 both events, weighted by the respective event probability: $\frac{1}{3}(\frac{1}{6}) + \frac{2}{3}(\frac{1}{8} + \frac{3}{8})$.

161 We next provide a general formula. We let a flow start at a vertex whose centrality we wish to compute,
 162 and at some point of the propagation process, a part f_u of the flow reaches u . Let \mathcal{N}_u be the neighborhood
 163 of interest given f_u , that is, the set of outgoing neighbors which have not yet been visited by the flow.
 164 Every outgoing edge (u, v) of u exactly corresponds to some outgoing neighbor v , so in what follows,
 165 we may refer to either one or the other. Let \mathcal{E}_u denote the set of possible outgoing edge subsets (where
 166 every edge (u, v) is represented by v the neighbor). We attach a possibly distinct probability $q(x)$ to every
 167 choice x in \mathcal{E}_u . Then $\sum_{x \in \mathcal{E}_u} q(x) = 1$.

168 Every x in \mathcal{E}_u corresponds to a set of edges (u, v) for v a neighbor. We further attach a weight $\omega_x(u, v)$
 169 to every edge in x , with the constraint that $\sum_{(u,v) \in x} \omega_x(u, v) = f_u$. For example, we could choose all edges
 170 with equal weight, that is $\omega_x(u, v) = \frac{f_u}{i}$ for every (u, v) in x containing i edges, to instantiate the special
 171 case where the flow is uniformly split among all edges.

For a given node u , we compute the expected flow from u to a chosen neighbor v . Every such choice
 of x comes with a probability $q(x)$, and every edge (u, v) in x has a weight $\omega_x(u, v)$, which sums up to

$$f_{uv} = \sum_{x \in \mathcal{E}_{u,v}} q(x) \omega_x(u, v), \quad (2)$$

172 where $\mathcal{E}_{u,v}$ contains the sets in \mathcal{E}_u themselves containing v .

173 **Example 1.** Consider the running example, with $u = v_1$. The set of neighbors of u is $\mathcal{N}_u = \{u, v_2, v_3, v_4\}$.
 174 We assign the following probabilities: $q(\{u\}) = q_1$, $q(\{v_2\}) = q_2$, $q(\{v_3\}) = q_3$, $q(\{v_4\}) = q_4$, $q(\{u, v_2\}) =$
 175 q_5 , $q(\{u, v_3\}) = q_6$, $q(\{u, v_4\}) = q_7$, $q(\{v_2, v_3\}) = q_8$, $q(\{v_2, v_4\}) = q_9$, $q(\{v_3, v_4\}) = q_{10}$, $q(\{u, v_2, v_3\}) =$
 176 q_{11} , $q(\{u, v_2, v_4\}) = q_{12}$, $q(\{u, v_3, v_4\}) = q_{13}$, $q(\{v_2, v_3, v_4\}) = q_{14}$, $q(\{u, v_2, v_3, v_4\}) = q_{15}$, with $\sum_{i=1}^{15} q_i =$
 177 1. We write down explicitly the terms involved in the sum (2) for two nodes, v_2 and v_3 :

$$\begin{aligned} f_{u,v_2} &= q_2 f_u + q_5 \omega_{\{u,v_2\}}(u, v_2) + q_8 \omega_{\{v_2,v_3\}}(u, v_2) + q_9 \omega_{\{v_2,v_4\}}(u, v_2) + q_{11} \omega_{\{u,v_2,v_3\}}(u, v_2) \\ &\quad + q_{12} \omega_{\{u,v_2,v_4\}}(u, v_2) + q_{14} \omega_{\{v_2,v_3,v_4\}}(u, v_2) + q_{15} \omega_{\{u,v_2,v_3,v_4\}}(u, v_2). \\ f_{u,v_3} &= q_3 f_u + q_6 \omega_{\{u,v_3\}}(u, v_3) + q_8 \omega_{\{v_2,v_3\}}(u, v_3) + q_{10} \omega_{\{v_3,v_4\}}(u, v_3) + \\ &\quad q_{11} \omega_{\{u,v_2,v_3\}}(u, v_3) + q_{13} \omega_{\{u,v_3,v_4\}}(u, v_3) + q_{14} \omega_{\{v_2,v_3,v_4\}}(u, v_3) + q_{15} \omega_{\{u,v_2,v_3,v_4\}}(u, v_3). \end{aligned}$$

178 Then $f_{u,u} + f_{u,v_2} + f_{u,v_3} + f_{u,v_4} = f_u \sum_{i=1}^{15} q_i = f_u$. By setting $q_8 = \frac{1}{3}$ and $\omega_{\{v_2,v_3\}}(u, v_2) = f_u \frac{2}{3}$, we find
 179 $f_{u,v_2} = f_u \frac{2}{9}$. Also, adding up $q_{10} = \frac{2}{3}$ and $\omega_{\{v_2,v_3\}}(u, v_3) = f_u \frac{1}{3}$, $\omega_{\{v_3,v_4\}}(u, v_3) = f_u \frac{1}{4}$, we find $f_{u,v_3} =$
 180 $f_u \frac{1}{9} + f_u \frac{1}{6} = f_u \frac{5}{18}$. Similarly $f_{u,v_4} = f_u \frac{1}{2}$ and indeed $f_u \frac{2}{9} + f_u \frac{5}{18} + f_u \frac{1}{2} = f_u$.

We repeat the computations for f_{v_3, v_5} and f_{v_4, v_5} . For that, we need to know what is f_{v_3} and f_{v_4} , but in this case, since both v_3 and v_4 only have one incoming edge, we have that $f_{v_3} = f_{v_1, v_3}$ and $f_{v_4} = f_{v_1, v_4}$:

$$f_{v_3, v_5} = \frac{1}{2}f_{v_3} = f_u \frac{1}{2} \frac{5}{18}, f_{v_4, v_5} = \frac{1}{2}f_{v_4} = f_u \frac{1}{2} \frac{1}{2}, f_{v_5} = f_{v_3, v_5} + f_{v_4, v_5} = f_u \frac{7}{18}.$$

It is true that by setting $f_u = 1$, we have $f_{u, v_2} = \frac{2}{9} = p_{u, v_2}$ as computed in Figure 3, but this is true because $p_{v_2, v_2} = 1$. If we consider v_3 instead, we find $f_{u, v_3} = \frac{5}{18} = 2p_{u, v_3}$, this is because we have computed what reaches v_3 , but since v_3 has an outgoing edge, we need to distinguish what stays from what continues. Notice that by setting $f_u = 1$ and $f_{v_3} = f_{v_4} = 1$, we get

$$f_{u, v_2} = \frac{2}{9}, f_{u, v_3} = \frac{5}{18}, f_{u, v_4} = \frac{1}{2}, f_{v_3, v_5} = \frac{1}{2}, f_{v_4, v_5} = \frac{1}{2}.$$

181 We then assign to edge (v_i, v_j) the probability f_{v_i, v_j} (with $f_u = 1$) as reported on Figure 3a.

The property of flow conservation observed in the example holds true in general, which we shall prove next. Indeed, when v varies in \mathcal{N}_u , the sets $\mathcal{E}_{u, v}$ appearing in the summation $\sum_{v \in \mathcal{N}_u} \sum_{x \in \mathcal{E}_{u, v}} q(x) \omega_x(u, v)$ may intersect, so for each choice x , one can gather all the $\mathcal{E}_{u, v}$ that contains x . For this x , we find a term in the above sum of the form $q(x) \sum_{(u, v) \in x} \omega_x(u, v) = q(x) f_u$. Then

$$\sum_{v \in \mathcal{N}_u} \sum_{x \in \mathcal{E}_{u, v}} q(x) \omega_x(u, v) = \sum_{x \in \mathcal{E}_u} q(x) f_u = f_u.$$

This shows that the flow from u to v is conserved over all the neighbors $v \in \mathcal{N}_u$ given f_u . Thus, by setting $f_u = 1$, the quantity

$$f_{uv} = \sum_{x \in \mathcal{E}_{u, v}} q(x) \omega_x(u, v)$$

182 becomes a probability, and in fact, putting this probability on the edge (u, v) in the context of the transfer
183 entropic centrality gives the same result as the above computations using the split-and-transfer model, as
184 in fact already illustrated on the figure in Example 1, since the probabilities displayed on the edges of the
185 graph have been computed in this manner. We summarized what we computed in the proposition below.

Proposition 1. *The split-and-transfer entropic centrality $C_{H, p}(u)$ of a vertex u is given by*

$$C_{H, p}(u) = - \sum_{v \in \mathcal{V}} q_{uv} \log_2(q_{uv})$$

186 where $q_{uv} = \sum_{x \in \mathcal{E}_{u, v}} q(x) \omega_x(u, v)$ is computed from (2) with $f_u = 1$ and the usual convention that $0 \cdot \log_2 0 =$
187 0 is assumed. The index p in $C_{H, p}$ emphasizes the dependency on the choice of the probability distribution
188 p . Then we have $C_{H, \text{unif}}$ when p is uniform as a particular case.

189 We thus showed that the split-and-transfer entropic centrality is equivalent to a transfer entropic
190 centrality, assuming the suitable computation of edge probabilities.

191 The notion of split-and-transfer entropic centrality characterizes the *spread* of a flow starting at u
192 through the graph. Now two vertices may have the same spread, but one vertex may be dealing with an
193 amount of goods much larger than the other. In order to capture the *scale* of a flow, we also propose a
194 scaled version of the above entropy.

195 **Definition 1.** The scaled split-and-transfer entropic centrality is accordingly given by $F(f_u)C_{H, p}(u)$
196 where F is a scaling function.

197 The scaling function F may depend on the nature of the underlying real world phenomenon being
198 modeled by the graph, with $F(f_u) = f_u$ being a simple default possible choice (other standard choices are
199 $F(f_u) = \sqrt{f_u}$ or $F(f_u) = \log(f_u)$). We use the default choice in the example below.

200 **Example 2.** Continuing with the same example, we use the edge probabilities as obtained in Example 1
201 to compute the transfer entropic centrality from Definition 1. The scaled entropic centralities of $u = v_1$
202 and v_3 are simply $f_u C_{H, p}(v_1) \approx f_u 1.9076$ and $f_{v_3} C_{H, p}(v_3) = f_{v_3} (\frac{1}{2} \log_2(2) + \frac{1}{2} \log_2(2)) = f_{v_3}$. Without
203 the scaling factor, $C_{H, p}$ is a measure of spread, and it makes sense that $C_{H, p}(v_1) > C_{H, p}(v_3)$. However
204 if v_1 is actually distributing some items in overall small amounts, while v_3 is not only getting this item
205 from v_1 but also producing it and furthermore sending it only to v_5 but in large amounts, then the scaling
206 factor could be used to refine the analysis and account for this extra information. From the moment
207 $f_{v_3} \geq 1.9076 f_{v_1}$, v_3 will be deemed more important than v_1 as per the scaled entropic centrality measure.

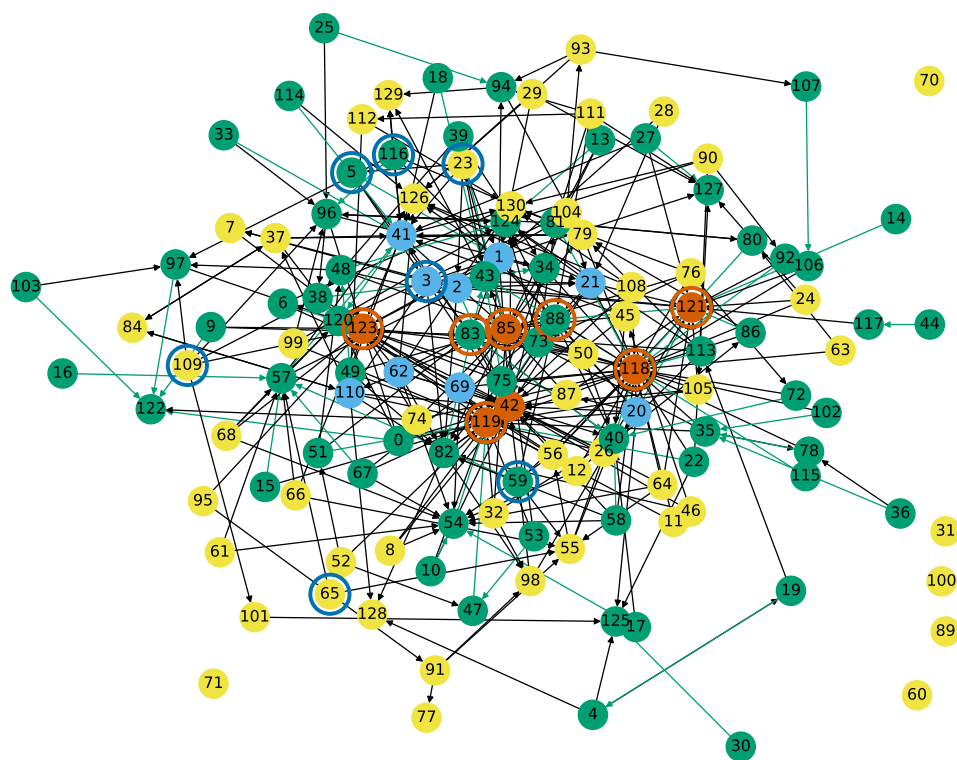


Figure 4. Cross-shareholding network of Tehran Stock Market companies: Vermillion and sky blue nodes have respectively the highest in- and out-degrees. Nodes circled in sky blue respectively vermilion have the highest entropic centrality under the current and reverse edge directionality.

3 CASE STUDIES

3.1 Shareholding in Tehran Stock Market

We next consider 131 companies from the Tehran Stock Market, as listed in Appendix A of Dastkhan and Gharneh (2016).¹ They form the vertices of a cross-shareholding network of companies which have shares of other companies. There is an edge between i and j if company i belongs to the investment portfolio of company j , i.e., j owns some share of i . Therefore the in-degree of node j is the number of companies that belong to the investment portfolio of company j . Conversely, the out-degree of node j is the number of companies that are shareholders of j . Edges are weighted, edge (i, j) has for weight the percentage of shares that company j has from company i . We will consider this graph, shown in Figure 4, and the graph with reverse edge directionality.

Nodes highlighted in green in Figure 4 have one edge with weight more than 0.5, meaning that more than 50% of their shares are owned by another company, otherwise they are in grey. Nodes highlighted in vermilion, superseding the other coloring, have the highest in-degrees, which means that they own shares of many other companies. They are nodes 121 (Adashare), 85 (NIKX1), 123 (Oilcopen), 42 (SA3A1), 119 (tamin org), and 118 (government). Nodes highlighted in sky blue have the highest out-degrees, which means that their shares are owned by many other companies (but possibly in small amounts). They are nodes 110 (BMEX1), 2 (CH12), 21 (FO041), 41 (GD021), 3 (GO02) with degree 7 and 69 (PFAX1), 1 (MADN), 20 (MS022) and 62 (PK061) with degree 8.

We next assign probabilities to edges. To do so, we use the edge weight, and fix the edge probability to be inversely proportional to its weight. As for the self-loops and their probability, they have a natural interpretation. Since the outgoing edges of node j indicate the companies that are shareholders of j , the self-loop refers to j still owning some of its own shares, and the amount is 100% minus what the other companies own (share ownerships with negligible amounts were not taken into account in the data set we used, so self-loops absorb these portions).

¹We thank the authors of Dastkhan and Gharneh (2016) for sharing their data with us.

Table 1. Vertices with the highest entropic centrality, their scaled entropic centrality, where f_u is the market size in percentage (their relative ranking is marked with subscript), their out-degrees (in the above part) or in-degrees (in the below part, for the graph with reverse edge directionality) and neighbors with the weight of the connecting edges. Bold face indicates a high degree. Ranks with respect to alpha/Katz (AK) with $\alpha = 1$, PageRank (PR) weighted (W) and unweighted (U), and betweenness (B).

no	ID	$C_{H,p}$	f_u	$f_u C_{H,p}$	out	neighbors	A/ K	PR(U /W)	B (W)
23	ARFZ1	3.1990	0.7153	2.2882 ₃	6	(1, 0.181), (2, 0.353), (5, 0.045), (43, 0.045) (41, 0.05), (85, 0.04)	1/ 1	1 /1	39
3	GO02	3.0205	0.9635	2.9103 ₁	7	(1, 0.224), (21, 0.099) (82, 0.011), (7, 0.037) (42, 0.028), (43, 0.377) (121, 0.185)	3/ 3	69 /69	3
109	IPAR1	2.9680	0.6874	2.0402 ₆	5	(96, 0.2), (101, 0.0963) (123, 0.173), (97, 0.078), (38, 0.139)	22/ 22	7 /4	39
59	PRDS1	2.9541	0.7951	2.3488 ₄	5	(88, 0.011), (57, 0.668), (118, 0.054), (55, 0.05) (82, 0.011)	14/ 14	18 /26	39
65	PK3A1	2.8857	0.6267	1.8084 ₇	2	(57, 0.42), (55, 0.206)	71/ 71	30 /12	39
5	KNRX	2.8817	0.9415	2.7131 ₂	3	(1, 0.8876), (3, 0.0209) (83, 0.033)	26/ 23	67 /37	31
116	PRSX1	2.8273	0.8086	2.2861 ₅	6	(96, 0.648), (97, 0.049) (88, 0.071), (41, 0.011) (129, 0.01), (79, 0.017)	8/ 7	12 /9	39
no	ID	$C_{H,p}$	f_u		in	neighbors			
118	gov	5.3434	9.8		40	(85, 0.1737)			
119	tamin org	4.6989	5.7647		31	(42, 0.0305)			
121	Adashare	4.4777	6.7827		17				
88	BTEJ1	4.2916	0.7143		9	(85, 0.474)			
123	Oilcopen	3.9154	3.5699		22				
83	TMEL1	3.8099	0.4849		9				
85	NIKX1	3.7693	0.9722		17				

232 Table 1 lists the seven nodes with the highest entropic centrality. The interpretation of entropic
 233 centrality here is that we are looking at the nodes whose shares are “most diversely owned” in terms
 234 of their shares being owned by different companies, whose shares are in turn themselves owned by
 235 others. The economic fortunes of the company whose centrality is looked at thus also affects those of the
 236 other companies, and the entropic centrality thus indicates the impact a particular company’s economic
 237 performance would have on the rest. We immediately see that this centrality measure is different from
 238 out-degree centrality. We can however look at how they relate, by considering the role of out-degrees
 239 not only on the nodes but also on their neighbors. We observe that only node 3 has one of the highest
 240 out-degrees, however, nodes 23 and 116 still have high out-degrees, but also are connected to neighbors
 241 which have high out-degrees, in fact, node 23 which has the highest entropic centrality has three high
 242 out-degree neighbors. For nodes 109 and 59, they still have a relatively high out-degree. For 5, it has a
 243 fairly low out-degree, but out of the 3 neighbors, two have high degrees themselves. The case of node 65
 244 is particularly interesting, since it has only two neighbors, namely 55 and 57. Neither of 55 nor 57 has
 245 a high centrality individually, but they together provide node 65 a conduit to a larger subgraph than the
 246 individual transit nodes themselves do, illustrating the secondary effects of flow propagation.

247 The cross-shareholding network of Tehran Stock Market was analyzed in Dastkhan and Gharneh
 248 (2016), where a closeness centrality ranking is shown to be almost identical to the degree based centrality

Table 2. Kendall rank correlation coefficient τ_K across the centralities for the Tehran stock exchange.

	$C_{H,p}$	alpha ($\alpha = 0.1$)	PageRank (UW) $\alpha = 0.85$	PageRank (W) $\alpha = 0.85$	Katz ($\alpha = 0.1$)
$C_{H,p}$	0	0.225935	0.318585	0.332645	0.225290
alpha	0.225935	0	0.31716	0.378709	0.004774
PageRank(UW)	0.318580	0.31716	0	0.131741	0.316
PageRank(W)	0.332645	0.378709	0.131741	0	0.377806452
Katz	0.225290	0.004774	0.316	0.377806	0

one. The entropic centrality ranking in contrast manages to capture a different dynamics, by involving the spread of influence via flow propagation, together with a quantitative edge differentiation.

The above approaches ignore any other information such as the market size share of the organizations. Arguably, between two organizations with identical position in the graph, the one with larger market size may be deemed to have larger influence on the other nodes. This is modeled by the scaled entropic centrality $C_H(u)f_u$, where f_u is the market size in percentage. We notice that this indeed creates a distinct relative ranking (indicated by subscript in Table 1, for example, ARFZ1 is ranked 3rd as per weighted entropic centrality). Particularly, among the top seven companies as per $C_H(u)$, we see that only PRDS1 continues to be in the same (fourth) rank. KNRX has the largest change in ranking, up from sixth to second. While the scaled entropic centrality ranking of the top two nodes are congruent with the ranking based solely on the scale factor (market size), we see that ARFZ1, which would be ranked 5th by market size, and first by solely network effect, is ranked 3rd when both factors are taken into account.

We compare the entropic centrality $C_{H,p}$ with respect to the alpha, Katz and PageRank centralities (using the reverse edge direction). Note that the unweighted graph has for largest eigenvalue $\lambda_1 \simeq 2.99715780$ (so $\frac{1}{\lambda_1} \simeq 0.3336494$). The ranking results for the most central entities from the Tehran stock exchange, and the overall Kendall tau rank correlation coefficients are reported in Tables 1 and 2 respectively. The entity 23 is outstandingly central with respect to all metrics but weighted betweenness. The alpha and Katz centralities are giving as expected very similar results, but they rank the entity 3 as third instead of second. They rank second the entity 20. A likely explanation could be that that 20 actually has a higher out-degree (and thus a higher in-degree in the reversed edge network) than entity 3. The top 7 most central entities have mostly a 0 betweenness (ranked 39), and are mostly ranked pretty low with respect to both versions of PageRank, weighted and unweighted. The most central entity for the weighted betweenness is 85, which is one of the most central with respect to in-degree (it has an in-degree of 18). Then 111 and 76 are second respectively for the unweighted and weighted PageRank. Entity 111 has out-neighbors 88,81,127,94,112 which become in-neighbors in the reversed edge graph, neither 111 itself nor its neighbors stand out by their degrees, however 76 has for in-neighbors in the reversed edge graph 72,73,130,85,118,76, and both 118 and 85 are very central with respect to in-degree, making it easier to explain why it is ranked high.

The Kendall rank correlation confirms that the entropic centrality differs from the other metrics not only to decide the most central vertices but also overall. The Kendall coefficient for unweighted betweenness has not been reported since only 38 vertices have a non-zero betweenness. This shows that the graph considered is far from being strongly connected. Overall, comparison points illustrate that the entropic centrality $C_{H,p}$ provides a new perspective not captured by the other algorithms.

We next consider the same graph but where edge directionality is reversed. A node becomes central if it owns diverse companies, which themselves may in turn own various companies. Since owning shares could be used to influence an organization's management, the entropic centrality based on reverse edges is thus a proxy indicator of how much control a specific entity has over the other entities in the market. Organizations with very high entropic centralities using either sense of edge direction could then be seen as probable candidates causing structural risks - be it by being 'too big to fail', or having too much control over significant portions of the market for it to be fairly competitive.

The nodes with highest entropic centrality are shown in Table 1. The most important one is the government: we expect it to be one of the most important players in Iran when it comes to owning shares in other companies (and yet not to appear in the list when the original edge direction is considered). We see a higher correlation between entropic centrality and in-degree than there was between entropic

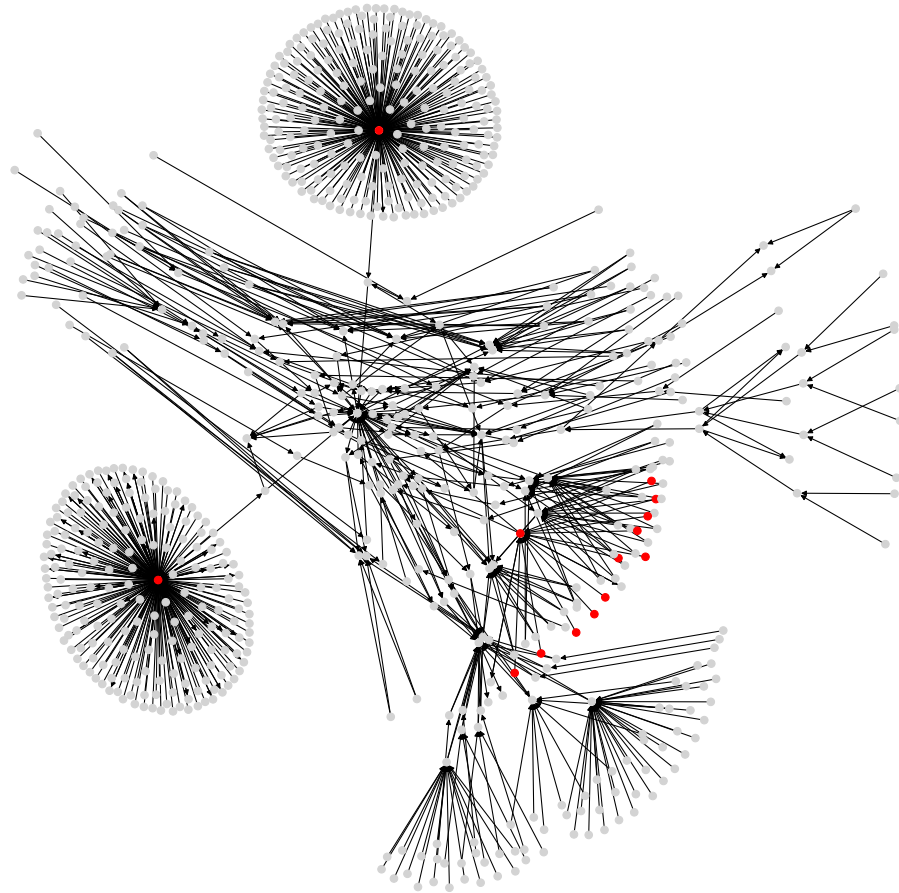


Figure 5. A subgraph of the Bitcoin subgraph, which comprises only addresses that have non-zero entropic centrality. Those in red are listed in Table 3, with the highest entropic centrality.

293 centrality and out-degree in Table 1. Among the seven most central nodes, five of them are having one of
 294 the highest in-degrees, the two most central nodes have themselves one high degree neighbor. Then node
 295 88 has a fairly low in-degree, but it is connected to node 85.

296 In summary, the case study of the Tehran stock exchange network exhibits three important intertwined
 297 aspects of our model. Firstly, it is flexible. It seamlessly captures the effect of relationships, considered
 298 either in a binary fashion (just the *structure*), or quantified with relative strengths (the *skew* in strength of
 299 the relationships), while it can also accommodate information which is intrinsic to the node but somewhat
 300 disentangled from the network (used as a *scale* factor). Second, reversing the edge direction gives a dual
 301 perspective. Finally, we see that we obtain different results and corresponding insights, based on which
 302 variations of the model is applied for a specific study. Naturally, figuring it out the best variation is done
 303 on a case-by-case basis.

304 3.2 A Bitcoin Subgraph

305 Our final case study is a subgraph of the Bitcoin wallet address network derived from Bitcoin transaction
 306 logs (see Figure 5). Bitcoin is a cryptocurrency Nakamoto (2008), and transactions (buy and sell) among
 307 users of this currency are stored and publicly available in a distributed ledger called blockchain. User
 308 identities are unknown, but each user has one or many wallet addresses, that are identifiers in every
 309 transaction. Then one transaction record amalgamates the wallet addresses of possibly several payers and
 310 payment receivers, together with the transaction amounts.

311 To be more precise, consider two Bitcoin transactions T_1 and T_2 . The transaction T_1 has n inputs, from
 312 wallet addresses A_1, \dots, A_n , of amounts i_{11}, \dots, i_{1n} respectively. The outputs, of amounts o_{11}, \dots, o_{1m}
 313 go to wallet addresses C_1, \dots, C_m respectively. The sum of inputs equals the sum of outputs and any
 314 transaction fees (say τ_1), i.e., $|T_1| = \sum_{k=1}^n i_{1k} = \tau_1 + \sum_{l=1}^m o_{1l}$. For the sake of simplicity, we will ignore

Table 3. Addresses with highest entropic centrality in the Bitcoin subgraph above (with the respective relative ranks as per other centralities - alpha/Katz with $\alpha = 0.1$ (AK), PageRank (PR), weighted (W) and unweighted (U)) and with highest centrality when edges have reverse directionality below.

address	$C_{H,p}$	f_u	out	$f_u C_H$	AK	PR (U/W)
3CD1QW6fjgTwKq3Pj97nty28WZAVkziNom	8.6633	0.0473	2807	652	1	1/1
38PjB1ghFrD9UQs7HV5n15Wt1i3mZP8Wke	5.7214	0.1961	382	481	3	14/14
3Eab4nDg6WJ5WR1uvWQirtMzWaA34RQk9s	5.4339	0.1778	568	514	2	13/15
3MYqQJ5LbDe9U3drsaDprKxWobVZA3UgAw	5.3316	0.9270	2	609	4	2/455
38mMQxz4knqfmeclW3atdygfWxvvnJfg7	5.3316	0.9268	2	3	4	2/3
33XZf8Ys9sbqnAKynA4yBckyzwN3SEZaU7	5.3316	0.9254	2	9	4	2/10
3P4C7jpF1oxHgxt4VgMRcCBEV3YEpaDUM	5.3316	0.9224	2	7	4	2/8
3Fp5ejYY8FsJ6Y3kb377VRjJunTeUVYsuq	5.3316	0.8966	2	2	4	2/3
3Q9SPyCN95szQUoQYgAHKgdhC3YnRsrFrW	5.3316	0.8928	2	8	4	2/8
38A6nGSMR59WHVnj9gaJ2Cm62y9kFE318i	5.3316	0.8908	2	5	4	2/6
3Ce7jUQn2RH5Ysdb4VvShoYymZLpkcqaAA	5.3316	0.8877	2	10	4	2/11
364qbSJFhwkBgZnMuhmUHdczpaZNS2PmE6	5.3316	0.8832	2	1	4	2/2
3KDgKr3qov4Ws5WPnaA2RHjcE1N2UeVYs3	5.3316	0.8619	2	4	4	2/5
1NxaBCFQwejSZbQfWcYNwgqML5wWoE3rK4	5.3316	0.1175	2	6	4	2/7

address	$C_{H,p}$	f_u	in
38PjB1ghFrD9UQs7HV5n15Wt1i3mZP8Wke	7.6477	171.359	218
3Eab4nDg6WJ5WR1uvWQirtMzWaA34RQk9s	7.5583	175.022	196
15hWpb3m5VXdn9KVsS4rSMnrQQJLhXVyN4	5.2649	7.50415	17
1C7PDYzjRDqomywDHEqx9huYoYQoGYgdV	4.9876	3.94921	31
1zksVRSDUuX2E5mMNvvaA9C4esfvVdfA	4.4176	0.49444	2

the transaction fees (i.e., consider $\tau_1 = 0$). A similar setting holds for transaction T_2 , where the same wallet address A_1 appears again as part of the inputs, together with some wallet addresses $B_2, \dots, B_{n'}$ which may or not intersect with A_2, \dots, A_n . By design, Bitcoin transactions do not retain an association as to which specific inputs within a transaction are used to create specific outputs.

Suppose one would like to create a derived address network from some extract of the Bitcoin logs of transactions, that is a graph whose nodes are Bitcoin wallet addresses, and edges are directed and weighted. There should be an edge from address u to address v if there is at least one transaction where some amount of Bitcoin is going from u to v . However as explained above, it is not always possible to disambiguate the input-output pairs. If the input amounts are particularly mutually distinct, and so are the output amounts, and there are input-output amounts that match closely, one might be able to make reasonable guess about matching a specific input to a specific output. In general, in absence of such particular information, one heuristic is to model the input-output association probabilistically. A common heuristic Kondor et al. (2014) is to consider that based on transaction T_1 there is an edge from A_1 to each of C_1, \dots, C_m . The same holds for transaction T_2 . Thus in the derived address network, there will be an edge from A_1 to each of the $C_1, \dots, C_m, D_1, \dots, D_{m'}$. If some outputs X, \dots, Z are in common to both transaction outputs, there is a single edge between A_1 and each of the addresses X, \dots, Z .

The derived address network gives us the graph to be analyzed, whose vertices are wallet addresses and edges are built as above. Originally, a given wallet address is sending Bitcoins to possibly different output wallet addresses within one transaction, and the same wallet address may be involved in different transactions, with possible reoccurrences of the same output addresses (this is the case of A_1 which is an input to both transactions T_1 and T_2 and X, \dots, Z appear as output transactions in both). In the split-and-transfer flow model, we can incorporate this information into the derived address network by assigning the probabilities $q(\{C_1, \dots, C_m\}) = \frac{i_{11}}{i_{11} + i_{21}}$ and $q(\{D_1, \dots, D_{m'}\}) = \frac{i_{21}}{i_{21} + i_{22}}$ with which the respective subsets $\{C_1, \dots, C_m\}$ and $\{D_1, \dots, D_{m'}\}$ of the set $\{C_1, \dots, C_m, D_1, \dots, D_{m'}\}$ of neighbors of A_1 are used. Other choices for $q(x)$ are possible, the rationale for this specific choice is to use a probability that is proportional to the amount of Bitcoin injected by A_1 in each of the transactions.

Edge weights in the derived address network are computed as follows. Let $|T_1| = \sum_{k=1}^m o_{1k}$ and

Table 4. Kendall rank correlation coefficient τ_K across the centrality algorithms for the Bitcoin subgraph dataset (excluding 3926 nodes which all had an entropic centrality score of zero).

	$C_{H,p}$	$f_u C_{H,p}$	alpha ($\alpha = 0.1$)	PageRank (UW)	PageRank (W)	Katz ($\alpha = 0.1$)
$C_{H,p}$	0	0.233172	0.235947	0.342135	0.395660574	0.234265
$f_u C_{H,p}$	0.233172	0	0.213537	0.315283	0.43371	0.211848
alpha	0.235947	0.213537	0	0.265286	0.49497	0.003209
PageRank(UW)	0.342135	0.315283	0.265286	0	0.429998	0.265253
PageRank(W)	0.395660	0.43371	0.49497	0.429998	0	0.496515
Katz	0.234265	0.211848	0.003209	0.265253	0.496515	0

$|T_2| = \sum_{k=1}^{m'} o_{2k}$ denote the total amounts involved in each of the transactions. For an edge between A_1 and C_l , which happens in T_1 , it is $\omega_{C_1, \dots, C_m}(A_1, C_l) = \frac{o_{1l}}{|T_1|}$, while for an edge between A_1 and D_l , which happens in T_2 , it is $\omega_{D_1, \dots, D_{m'}}(A_1, D_l) = \frac{o_{2l}}{|T_2|}$. We thus have

$$\sum_{l=1}^m \omega_{C_1, \dots, C_m}(A_1, C_l) = \sum_{l=1}^m \frac{o_{1l}}{|T_1|} = 1, \quad \sum_{l=1}^{m'} \omega_{D_1, \dots, D_{m'}}(A_1, D_l) = \sum_{l=1}^{m'} \frac{o_{2l}}{|T_2|} = 1.$$

341 If some node pairs, and thus edges, repeat across transactions (for example, A_1 to X, \dots, Z in our example),
 342 these edge weights should cumulate in the overall derived address network. This is captured by the
 343 formula (2) which is here instantiated as

$$\begin{aligned} f_{A_1, X} &= q(\{C_1, \dots, C_m\}) \omega_{C_1, \dots, C_m}(A_1, X) + q(\{D_1, \dots, D_{m'}\}) \omega_{D_1, \dots, D_{m'}}(A_1, X) \\ &= \frac{i_{11}}{i_{11} + i_{21}} \frac{o_{1x}}{|T_1|} + \frac{i_{21}}{i_{11} + i_{21}} \frac{o_{2x}}{|T_2|} \end{aligned}$$

344 where in transaction T_1 the output to address X is o_{1x} , while it is o_{2x} in transaction T_2 .

345 In a departure from previous works that derive the address network in a manner explained above
 346 Kondor et al. (2014), our graph model is able to retain the information that subsets of edges co-occur, or
 347 not, as displayed above. For that reason, the Bitcoin address network is a natural candidate (and in fact,
 348 part of the inspiration) for the general flow model with arbitrary splits and transfers as considered in this
 349 paper, where individual flows may go through a subset of outgoing edges.

350 While we would like to emphasize that we use here this Bitcoin graph to explore the entropic centrality
 351 model, it may still be worth mentioning that one identified suspect node from another of our study
 352 Phetsouvanh et al. (2018), namely node 15hWpb3m5VXd9n9KVvS4rSMnrQQJLhXVvYn4, has high
 353 enough entropic centrality to be listed (see Table 3 below) as a top entropic centrality node. Thus, the
 354 entropic centrality analysis can be used as a tool to identify nodes of interest, and to create a shortlist of
 355 nodes to be investigated further in detail, in the context of Bitcoin forensics.

356 Tables 3 and 4 compare the entropic centrality $C_{H,p}$ with other centralities. With respect to scaled
 357 entropic centrality, there is a large variation in the weightages associated with the edges, which has
 358 a significant impact on the relative rankings between scaled/unscaled entropic centralities. With re-
 359 spect to weighted betweenness, only three addresses are relevant, they are, with their respective in-
 360 and out-degree, 3Eab4nDg6WJ5WR1uvWQirtMzWaA34RQk9s (ranked 1, in-degree: 196, out-degree:
 361 568), 38PjB1ghFrD9UQs7HV5n15Wt1i3mZP8Wke (ranked 2, in-degree: 218, out-degree: 382), and
 362 3CD1QW6fjgTwKq3Pj97nty28WZAVkziNom (in-degree: 14, out-degree: 2807). The other addresses are
 363 ranked 69 (corresponding to a betweenness of 0). The graph has for largest eigenvalue $\lambda_1 \simeq 7.1644140$
 364 and $\frac{1}{\lambda_1} \simeq 0.139578$. As with the previous cases, alpha and Katz centralities are very close to each other,
 365 they also agree more closely with $C_{H,p}$ on the most central addresses, but Table 4 shows that this is not the
 366 case in general. The trends shown by the Kendall rank correlation coefficient is similar to previous cases:
 367 there are more dissimilarities between PageRank and entropic centralities than between alpha/Katz and
 368 entropic centralities, but overall, entropic centralities give a different view point, as would be expected by
 369 extrapolating Borgatti's view point.

370 4 CONCLUSIONS

371 In this paper, we studied the concept of entropic centrality proposed by Tutzauer (2007), which originally
372 determined the importance of a vertex based on the extent of dissemination of an indivisible flow
373 originating at it, by considering the uncertainty in determining its destination. We extended this concept
374 to model divisible flows, which better reflect certain real world phenomenon, for instance, flows of money.
375 In fact, one of the motivating scenarios that prompted us to study this model was to study the network
376 induced by Bitcoin transactions - though, in the course of the work, and to validate the model, we also
377 identified and analyzed other use cases, with arbitrary divisions of the flow. A previous work which
378 considered only equitable divisions of the flow was shown to be a special case of the general model
379 studied in this paper.

380 The flow based entropic centrality model bears in spirit some similarity with eigenvector based
381 centrality measures in the sense that the importance of vertex node is determined by taking into account a
382 transitive effect, namely, connections to a central vertex contributes to increase the centrality. We thus
383 compared our approach with several representatives of this family, specifically alpha centrality, PageRank
384 and Katz centrality. We observed that alpha and Katz centralities are closer to entropic centralities than
385 PageRank (in terms of Kendall tau distance), but they are still fairly different. This could be extrapolated
386 from the view point of Borgatti (2005), which advocates to use path based centrality for transfer type
387 of flow, and not eigenvector based centralities, which are best suited for duplication. This indicates that
388 the new entropic centrality provides novelty not only in the principled manner in which it captures the
389 phenomenon of divisible flows, but also in terms of the results and associated insights obtained from it.

390 REFERENCES

- 391 Benzi, M. and Klymko, C. (2015). On the limiting behavior of parameter-dependent network centrality
392 measures. *SIAM Journal on Matrix Analysis and Applications*, 36(2):686–706.
- 393 Bonacich, P. (1972). Factoring and weighting approaches to status scores and clique identification. *Journal*
394 *of Mathematics Sociology*, 2:113–120.
- 395 Bonacich, P. and Lloyd, P. (2001). Eigenvector-like measures of centrality for asymmetric relations.
396 *Social networks*, 23(3):191–201.
- 397 Borgatti, S. P. (2005). Centrality and network flow. *Social Networks*, 27:55–71.
- 398 Dastkhan, H. and Gharneh, N. S. (2016). Determination of systematically important companies with
399 cross-shareholding network analysis: A case study from an emerging market. *International Journal of*
400 *Financial Studies*.
- 401 Estrada, E. (2011). *The Structure of Complex Networks: Theory and Applications*. Oxford University
402 Press.
- 403 Fan, R., Xu, K., and Zhao, J. (2017). A gpu-based solution for fast calculation of the betweenness
404 centrality in large weighted networks. *PeerJ Computer Science*, 3:e140.
- 405 Katz, L. (1953). A new status index derived from sociometric analysis. *Psychometrika*.
- 406 Kondor, D., Pósfai, M., Csabai, I., and Vattay, G. (2014). Do the rich get richer? an empirical analysis of
407 the bitcoin transaction network. *PLoS ONE*, 9(2).
- 408 Nakamoto, S. (2008). *Bitcoin: A Peer-to-Peer Electronic Cash System*.
- 409 Newman, M. (2009). The mathematics of networks. *The New Palgrave Encyclopedia of Economics*.
- 410 Nikolaev, A. G., Razib, R., and Kucheriya, A. (2015). On efficient use of entropy centrality for social
411 network analysis and community detection. *Social Networks*, 40.
- 412 Oggier, F., Silivanxay, P., and Datta, A. (2018). Entropic centrality for non-atomic flow network. In
413 *International Symposium on Information Theory and its Applications (ISITA)*.
- 414 Opsahl, T., Agneessens, F., and Skvoretz, J. (2010). Node centrality in weighted networks: Generalizing
415 degree and shortest paths. *Social Networks*, 32.
- 416 Page, L., Brin, S., Motwani, R., and Winograd, T. (1999). *The PageRank citation ranking: Bringing order*
417 *to the web*.
- 418 Phetsouvanh, S., Oggier, F., and Datta, A. (2018). Egret: Extortion graph exploration techniques in the
419 bitcoin network. In *IEEE ICDM Workshop on Data Mining in Networks (DaMNet)*.
- 420 Tutzauer, F. (2007). Entropy as a measure of centrality in networks characterized by path-transfer flow.
421 *Social Networks*, 29.